

## Healing of surgical and burn wounds with dressings containing propolis/hyaluronic acid/starch/polyurethane

Poodineh Haji Poor F.<sup>\*</sup>, Feyz Bakhsh A. PhD<sup>\*\*</sup>  
Malek Nia L. PhD<sup>\*\*\*</sup>, Ahanian I. PhD<sup>\*\*\*\*</sup>

### Abstract:

Biological macromolecules, such as polysaccharides and proteins, are considered ideal options for use in skin tissue engineering, both in vitro and in vivo, due to their suitable biocompatibility and biodegradability. Despite numerous studies that have been conducted in this area, there is a need to construct a scaffold with antibacterial properties and desirable biocompatibility. The aim of this study is to construct and evaluate a core-shell electrospun scaffold for skin tissue engineering. In this structure, polyurethane acts as the shell, and a mixture of starch, propolis extract, and hyaluronic acid forms the core. The morphology of the scaffold was determined using scanning electron microscopy and transmission electron microscopy. The physical and mechanical properties of the scaffold, including contact angle, Young's modulus, and strain at break, were evaluated. The antibacterial activity of the scaffold against *Staphylococcus aureus* and *Escherichia coli* was investigated. The cytotoxicity of the scaffold was evaluated using L929 fibroblast cells. The effectiveness of the scaffold in wound healing under in vivo conditions was also investigated. Microscopic images showed that the core-shell structure was successfully formed. The contact angle of the scaffold was 56.7 degrees, indicating suitable hydrophilic properties for cell attachment. Mechanical tests showed a Young's modulus of 8.12 MPa and a strain at break of 46%, indicating an optimal balance between mechanical strength and flexibility. The scaffold exhibited strong antimicrobial activity against *Staphylococcus aureus* and *Escherichia coli*. Cytotoxicity evaluations showed no toxicity, and the adhesion and proliferation of L929 fibroblast cells on the scaffold were increased. Studies conducted under in vivo conditions confirmed the potential of the scaffold in tissue engineering and showed wound healing. The results of this study show that the electrospun scaffold with a polyurethane shell and a starch/propolis extract/hyaluronic acid core is a versatile and promising platform for advanced applications in skin tissue engineering and regenerative medicine.

**Keywords:** skin tissue engineering, hyaluronic acid, polyurethane, starch

\*PhD student in Biomedical Engineering, Department of Biomedical Engineering, Kish Branch, Islamic Azad University, Kish, Iran

\*\*Assistant Professor, Department of Chemistry, Central Tehran Branch, Islamic Azad University, Tehran, Iran

\*\*\*Assistant Professor, Department of Biomedical Engineering, South Tehran Branch, Islamic Azad University, Tehran, Iran

\*\*\*\*Assistant Professor, Department of Electrical Engineering, South Tehran Branch, Islamic Azad University, Tehran, Iran

Received: 12/10/2024

Accepted: 11/03/2025

**Corresponding Author: Dr. Alireza Feyz Bakhsh**

Tel: 05433222508

E-mail: Ali.fb1973@yahoo.com

## Background and Objective

The skin, the largest organ in the human body, plays a vital role in protecting internal organs from various environmental threats, including physical, chemical, and mechanical damage.<sup>1,2</sup> Additionally, it acts as the outermost layer for oxygen exchange with the environment, delivering sufficient oxygen to underlying tissues.<sup>3-8</sup> The skin also facilitates the elimination of toxins through perspiration. If damaged, wounds develop, and if left untreated, they can lead to necrosis.<sup>9-13</sup>

Electrospinning is a versatile technique in skin tissue engineering that enables the fabrication of nanofibrous scaffolds mimicking the extracellular matrix, enhancing cell adhesion, proliferation, and differentiation.<sup>14,15</sup> These scaffolds can be loaded with bioactive agents, such as growth factors or antimicrobial compounds, to improve wound healing and tissue regeneration.<sup>16,17</sup> The high surface area of electrospun fibers and their tunable properties make them ideal candidates for advanced wound care and skin regeneration therapies.<sup>18-20</sup> Starch, a natural, abundant, and low-cost polymer, is highly biocompatible and biodegradable, making it a valuable material in tissue engineering.<sup>20-23</sup> Studies have shown that starch enhances cell proliferation, adhesion, and differentiation, significantly aiding in wound healing. Recent advances in electrospinning have enabled the fabrication of starch-based scaffolds, although challenges persist due to the branched structure of amylopectin in starch, which complicates fiber formation.<sup>24-27</sup> Despite these challenges, researchers continue to explore the potential of starch-based nanofiber scaffolds. However, starch has certain limitations in electrospinning, including poor mechanical strength, thermal instability, hydrophobicity, and processing difficulties, which have been addressed in various studies.<sup>25,28-30</sup>

Polyurethanes, polymers consisting of urethane groups formed from the reaction between isocyanates and alcohol groups, are attractive due to their versatile physical and biological properties.<sup>18,19</sup> Despite the

advantages of these polymers, their slow degradation rate and relatively low biocompatibility have limited their application in skin tissue engineering.

Hyaluronic acid, another natural polysaccharide, is composed of repeating disaccharide units and is found in most animal tissues, where it exists as a highly viscous solution.<sup>31,32</sup> Hyaluronic acid plays a crucial role in the structure and organization of the extracellular matrix, helping to maintain extracellular spaces, transport ions and nutrients, and support tissue hydration.<sup>33</sup>

Furthermore, propolis extract, a natural resinous substance rich in bioactive compounds such as flavonoids, phenolic acids, and terpenoids, exhibits potent antioxidant, anti-inflammatory, and antimicrobial properties in tissue engineering, particularly for starch. These components promote faster healing by stimulating cell proliferation, enhancing collagen synthesis, and reducing inflammation, making it an excellent candidate for regenerative applications.<sup>34,35</sup>

Core-shell electrospinning is a technique that enables the fabrication of nanofibers with small diameters at the nanoscale, thereby producing porous and three-dimensional scaffolds resembling the extracellular matrix.<sup>17,36-38</sup> These scaffolds are highly relevant to starch, as their porosity supports oxygen and moisture exchange, which is essential for tissue regeneration.<sup>39</sup> When the viscosity of the electrospinning solution is low, a mixture of several polymers can be used, or alternatively, core-shell electrospinning can be employed to coat one polymer with another. This method allows the use of separate solutions without a common solvent. It also enables the controlled release of two drugs or bioactive agents simultaneously.<sup>40-45</sup> In summary, the aim of this research is to develop a novel scaffold using core-shell electrospinning with desirable properties (biocompatibility, suitable mechanical properties, antibacterial activity, and wound-healing ability) for

application in skin tissue engineering and skin wound repair.

Specifically, the objectives of this research were:

**Fabrication of Core-Shell Scaffold:** To create a scaffold using the core-shell electrospinning method, where polyurethane forms the shell and a combination of starch, propolis extract, and hyaluronic acid forms the core.

**Scaffold Characterization:** To investigate the physical, chemical, and mechanical properties of the fabricated scaffold. This includes evaluating morphology, hydrophilicity (contact angle), mechanical strength (Young's modulus and strain at break), and other relevant characteristics.

**Evaluation of Antibacterial Properties:** To assess the scaffold's ability to inhibit the growth of harmful bacteria commonly found in skin infections, particularly *Staphylococcus aureus* and *Escherichia coli*.

**Cytotoxicity Assessment:** To determine whether the scaffold is toxic to human cells. This was conducted using L929 fibroblast cells, and the degree of cell adhesion and proliferation on the scaffold was examined.

**Evaluation of Wound Healing Efficacy (In Vivo):** To investigate the potential of the scaffold to accelerate the wound healing process in an animal model (in vivo studies).

## Materials and Methods

This study investigates the potential of core-shell electrospun scaffolds in the repair of surgical and burn wounds. This research was conducted in two phases, *in vitro* and *in vivo*, with the aim of comparing the effectiveness of different scaffolds with varying compositions in the wound healing process.

In the *in vivo* section, female Wistar rats were used as the study population. These rats were divided into three groups, each consisting of six samples: group one (polyurethane/starch scaffold), group two (polyurethane/starch/hyaluronic acid scaffold), and group three (polyurethane/starch/hyaluronic acid-propolis scaffold). In

the *in vitro* section, mouse L929 fibroblast cells were used.

The methods employed in this study include the following steps: First, core-shell electrospun scaffolds were fabricated using the core-shell electrospinning method with various compositions of polyurethane, starch, hyaluronic acid, and propolis. These scaffolds were then characterized using various techniques. Scanning electron microscopy (SEM) and transmission electron microscopy (TEM) were used to evaluate morphology, spectroscopy was used to determine chemical composition, a tensile testing machine was used to measure mechanical properties (Young's modulus and strain at break), and calorimetry was used to determine thermal properties. Additionally, the water contact angle was measured to determine hydrophilicity, and water absorption and weight loss were measured to evaluate scaffold absorption and degradation in phosphate-buffered saline solution. The antibacterial activity of the scaffolds was also evaluated using the zone of inhibition test against *Staphylococcus aureus* and *Pseudomonas aeruginosa* bacteria.

Subsequently, *in vitro* tests were performed, including culturing L929 fibroblast cells on the scaffolds and measuring cell viability using the cell metabolic activity assay. Cell adhesion was also observed using scanning electron microscopy. The *in vivo* study was conducted on rats with the following design:

- Group 1) Polyurethane/starch: Rats whose wounds were treated with polyurethane/starch scaffolds.
- Group 2) Polyurethane/ starch/ hyaluronic acid: Rats whose wounds were treated with polyurethane/starch/hyaluronic acid scaffolds.
- Group 3) Polyurethane/ starch/ hyaluronic acid-propolis: Rats whose wounds were treated with polyurethane/starch/ hyaluronic acid-propolis scaffolds.
- Control group: Wounds created in rats were treated with sterile gauze (standard dressing).

Each group consisted of 6 rats. In the *in vivo* phase, circular wounds were created on the dorsal skin of the rats and treated with the fabricated scaffolds or sterile gauze (control group). The extent of wound healing was evaluated by measuring the wound diameter on days 1, 7, and 14. Finally, skin tissue samples were examined histologically using light microscopy after hematoxylin and eosin staining. Data were statistically analyzed using one-way analysis of variance (ANOVA).

## 2.1 Preparation of polyurethane/starch/hyaluronic acid propolis

Initially, polyurethane was dissolved in dimethylformamide at a 12% weight ratio. Under magnetic stirring at 25°C, this resulted in a clear and homogeneous solution. Separately, 9% by weight starch was completely dissolved in distilled water at 90°C. Subsequently, hyaluronic acid (1% by weight) and propolis (1% by weight) were dissolved at 25°C and added to the starch solution.

For the core-shell structure, polyurethane was chosen as the shell, and starch, hyaluronic acid, and propolis were chosen as the core materials, respectively. The solutions of polyurethane, polyurethane/starch, polyurethane/starch-hyaluronic acid, and polyurethane/starch/hyaluronic acid-propolis were loaded into separate syringes connected to a core-shell electrospinning device. The flow rates were controlled independently using syringe pumps. The diameters of the inner and outer needles were 0.2 mm and 0.6 mm, respectively. The electrospun scaffolds were collected on aluminum foil. The collectors were dried at room temperature (25°C) for 24 hours.

The following steps were performed to crosslink the core-shell structures using glutaraldehyde vapor (20% aqueous solution) for 24 hours to increase water resistance. After crosslinking, the structures were thoroughly washed with double-distilled water to remove excess glutaraldehyde and then dried in a vacuum oven at 60°C for 4 hours.

The following text pertains to the evaluation and characterization of the fibrous scaffolds:

## 2.2 Description of fibrous scaffolds

### 2.2.1 Morphology assessment

The morphology of the electrospun scaffolds was examined using scanning electron microscopy (SEM) at a voltage of 15 kV. The samples were mounted on metal stubs using double-sided adhesive tape and coated with a nanoscale layer of gold via sputtering. The fiber diameter and distribution were analyzed using ImageJ software, with the average calculated from 100 measured fibers.

Transmission electron microscopy (TEM) was used to confirm the core-shell structure. Carbon-coated copper grids were placed on the collector during electrospinning, and a single layer of fibers was deposited for TEM analysis.

### 2.2.2 Fourier Transform Infrared Spectroscopy (FTIR-ATR)

Attenuated total reflectance Fourier transform infrared spectroscopy (FTIR-ATR) was employed to analyze the chemical composition of the scaffolds. Spectra were recorded in the range of 400 to 4000  $\text{cm}^{-1}$ , using a single-reflection setup with a diamond crystal. A total of 64 scans were collected with defined resolution, and water and carbon dioxide corrections were applied.

### 2.2.3 Mechanical Evaluation

Mechanical properties were assessed using a tensile testing machine with a 50 N load cell at room temperature. Samples with dimensions of 30 × 10  $\text{mm}^2$  (n=6) were tested at a crosshead speed of 5 mm/min. Tensile stress and strain at break were recorded and measured.

### 2.2.4 Thermal Evaluation

The thermal behavior of the scaffolds was evaluated using differential scanning calorimetry (DSC). The test was performed from 25°C to 600°C with a heating rate of 10°C/min to determine the effect of hyaluronic acid (hydroxyapatite) and

propolis (polyethylene) on the thermal stability of the scaffolds.

### 2.2.5 Contact Angle Measurement

Water contact angle measurements were performed using the sessile drop method. A 0.5  $\mu\text{L}$  drop of water was placed on each of the 6 samples, and the water contact angle was recorded after 15 seconds at room temperature to evaluate the hydrophilicity of the scaffolds.

### 2.2.6 Water Absorption and Weight Loss Measurement

Scaffolds with dimensions of  $10 \times 10 \text{ mm}^2$  were immersed in phosphate-buffered saline (PBS, pH 7.4) for 24 hours at room temperature to measure water absorption. The scaffolds were weighed before immersion and after incubation, and the percentage of water absorption was calculated using the following equation:

$$\text{WU (\%)} = (W_t - W_0) / W_0 \times 100 \text{ (Equation 1-2)}$$

This equation calculates the percentage increase in weight due to water absorption.

To measure weight loss, scaffolds with dimensions of  $10 \times 10 \text{ mm}^2$  were placed in phosphate-buffered saline (PBS) for 28 days. The samples were weighed before and after drying to calculate the degradation rate using the following equation:

$$\text{Weight Loss (\%)} = (W_i - W_d) / W_d \times 100 \text{ (Equation 2-2)}$$

### 2.2.7 Antibacterial Activity

The antibacterial activity of the samples against *Pseudomonas aeruginosa* (Gram-negative) and *Staphylococcus aureus* (Gram-positive) bacteria was tested using the zone of inhibition method. In this method, samples containing polyethylene and samples without it were placed on nutrient agar plates previously inoculated with bacteria. The plates were then incubated overnight at an appropriate temperature.

After incubation, the zones of bacterial growth inhibition were measured, and the results were recorded as mean  $\pm$  standard deviation. These measurements allow the

analysis and comparison of the antibacterial effects of different materials, with or without propolis, on bacterial growth.

The results obtained from this experiment can aid in evaluating the antibacterial capabilities of the scaffolds and may contribute to the development of new materials for medical applications.

### 2.3 Cell adhesion test

Mouse fibroblasts (L929 cells) were cultured on the scaffolds to evaluate cell adhesion and proliferation. The electrospun scaffolds were sterilized with 70% ethanol and ultraviolet radiation. Fibroblast cells ( $1 \times 10^5$  cells/well) were seeded onto the scaffolds in a 24-well plate and incubated at  $37^\circ\text{C}$  with 5% carbon dioxide. The cell viability assay was performed on days 1, 3, and 7 to evaluate cell viability. Absorbance was measured using a BioTek microplate reader.

For scanning electron microscopy (SEM) analysis, the cells were fixed with 3% glutaraldehyde and dehydrated with ethanol solutions of varying concentrations (50% to 100%). The scaffolds were treated with hexamethyldisilazane and dried in a vacuum oven for 24 hours before SEM observation.

### 2.4 In Vivo Studies

Animal experiments were conducted following previous studies.<sup>40</sup> Rats (6-8 weeks old, 180-200 g) were divided into three groups of two: polyurethane/starch, polyurethane/starch/hyaluronic acid. Circular wounds (18 mm diameter) were created on the dorsal skin of the rats under anesthesia. The wounds were treated with scaffolds or sterile gauze (control) and monitored for healing for 1, 7, and 14 days using a digital caliper.

#### 2.4.1 Histological Evaluation

On day 14, the rats were sacrificed, and skin samples were fixed in 10% formalin for 24 hours. Sections (4  $\mu\text{m}$  thick) were prepared, stained with hematoxylin and eosin, and examined under a digital light microscope.

### 2.5 Statistical Analysis

Statistical analyses were performed using IBM SPSS Statistics 27.0.1 software and one-way analysis of variance (ANOVA). Data were reported as mean  $\pm$  standard deviation. In this study, p-values  $< 0.05$  were considered to indicate a statistically significant difference between groups.

## Discussion and Conclusion

### 3.1 Morphological Characteristics

Four nanofibrous scaffolds were successfully fabricated using optimized electrospinning parameters. Scanning electron microscopy (SEM) micrographs of the prepared scaffolds are presented in Figure 1A. As shown in Figure 1(B) and Table 1, the addition of starch reduced the fiber diameter from  $836 \pm 172$  nm (for pure polyurethane) to  $612 \pm 93$  nm. SEM

micrographs in Figure 1(D) and Table 1 demonstrate the effect of adding propolis to the core structure. The polyurethane/starch/hyaluronic acid-propolis electrospun scaffold showed a significant decrease in fiber diameter, with an average of  $382 \pm 37$  nm, and greater porosity compared to the polyurethane/starch and polyurethane/starch scaffolds. As seen in Table 1, the scaffolds had fully interconnected pores, with average pore sizes for polyurethane, polyurethane/starch, polyurethane/starch, and polyurethane/starch/hyaluronic acid-propolis scaffolds of  $1.25 \pm 0.2$ ,  $1.734 \pm 0.2$ ,  $3.186 \pm 0.4$ , and  $3.674 \pm 0.3$   $\mu\text{m}$ , respectively. The porosity of the scaffolds was analyzed using MATLAB software, and the results are presented in Table 1.

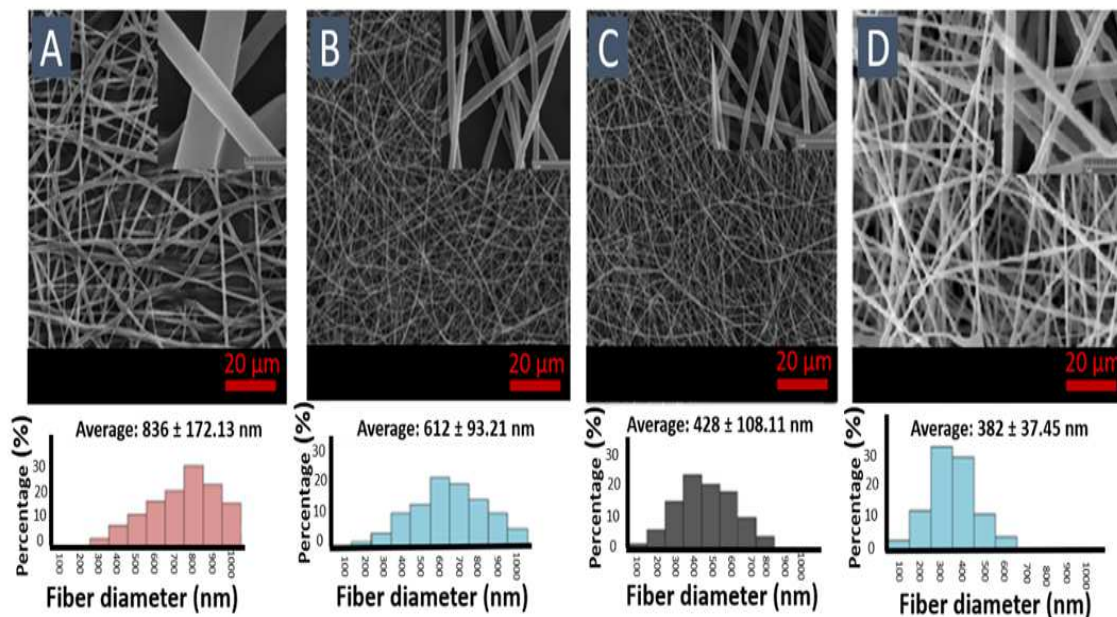


**Figure 1- Scanning electron microscope images of electrospun fibers: (a) polyurethane, (b) polyurethane/starch, (c) polyurethane/starch, and (d) polyurethane/starch/hyaluronic acid-propolis samples.**

**Table 1- Textural properties of electrospun fibers**

<i>sample</i>	<i>Average diameter size (nm)</i>	<i>Average pore size (<math>\mu\text{m}</math>)</i>	<i>Porosity percentage</i>
<i>Polyurethane</i>	$172 \pm 836$	$0.2 \pm 1.25$	83
<i>Polyurethane/starch</i>	$93 \pm 612$	$0.2 \pm 1.734$	83
<i>Polyurethane/starch/hyaluronic acid</i>	$108 \pm 428$	$0.4 \pm 3.186$	83
<i>Polyurethane/starch/hyaluronic acid – propolis</i>	$37 \pm 382$	$0.3 \pm 3.674$	83

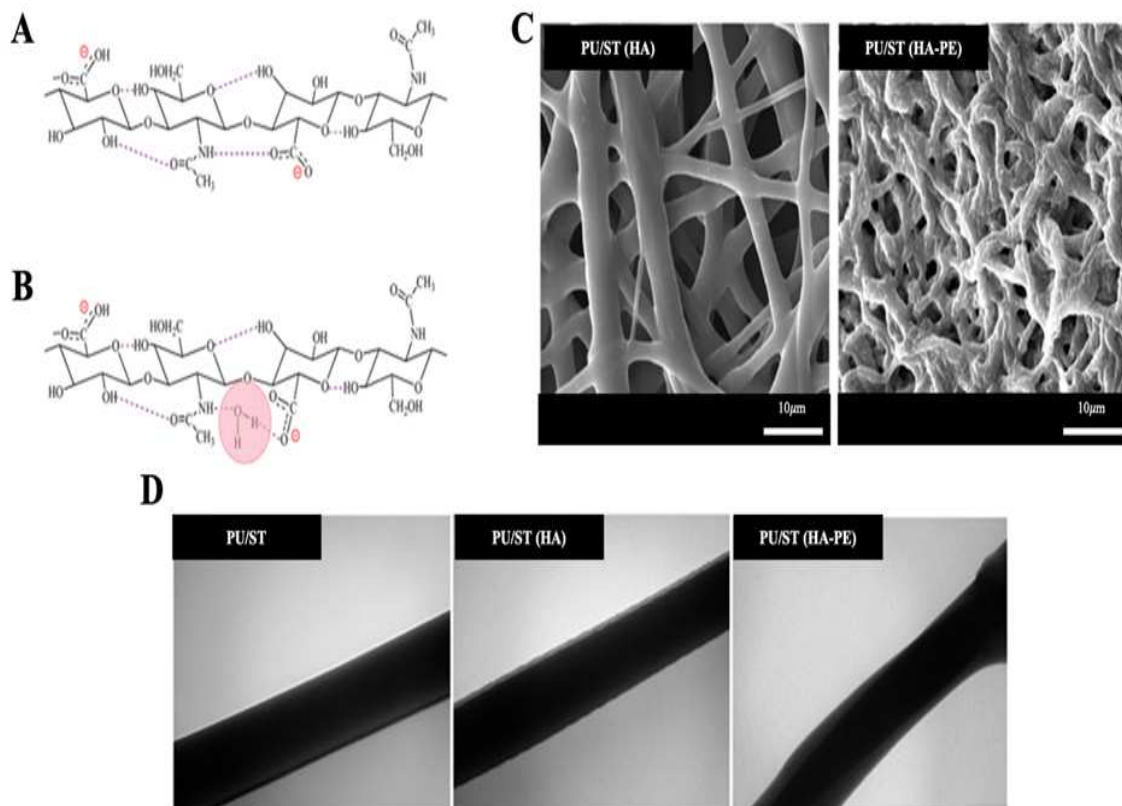


**Figure 2- a) Chemical structure of hyaluronic acid. b) Chemical structure of hyaluronic acid dissolved in distilled water. c) Scanning electron microscope image of polyurethane/starch and polyurethane/starch/hyaluronic acid-propolis core-shell scaffolds after crosslinking. d) Images of nanofibers showing the core-shell structure of polyurethane/starch, polyurethane/starch and polyurethane/starch/hyaluronic acid-propolis.**

**Table 2- Mechanical tensile properties of electrospun fibers.**

<i>sample</i>	<i>Elastic modulus (MPa)</i>	<i>Tensile strength (MPa)</i>	<i>Strain at failure(%)</i>
<i>Polyurethane</i>	<i>0.12±5.67</i>	<i>0.57±13.81</i>	<i>32±320</i>
<i>Starch</i>	<i>0.08±1.81</i>	<i>0.12±5.83</i>	<i>2±18</i>
<i>Polyurethane/starch</i>	<i>0.14±3.35</i>	<i>0.17±7.93</i>	<i>28±58</i>
<i>Polyurethane/starch/hyaluronic acid</i>	<i>0.17±3.23</i>	<i>0.28±7.18</i>	<i>19±62</i>
<i>Polyurethane/starch/hyaluronic acid – propolis</i>	<i>0.21±4.13</i>	<i>0.21±8.12</i>	<i>12±46</i>

### 3.2 ATR-FTIR

ATR-FTIR spectroscopy was used to identify the polymeric components and additives in the electrospun scaffolds (Figure 3(A)).

### 3.3 Mechanical Properties

Table 2 and Figure 3(B) summarize the tensile strength, strain at break, and Young's modulus for electrospun scaffolds of polyurethane, starch, polyurethane/starch, polyurethane/starch with hyaluronic acid, and polyurethane/starch with both hyaluronic acid and propolis. The mechanical properties of the polyurethane scaffold showed a tensile strength of  $13.81 \pm 0.57$  MPa and a strain at break of  $320 \pm 32\%$ . In contrast, the tensile strength and strain at break for the starch scaffold were  $5.83 \pm 0.12$  MPa and  $18 \pm 2\%$ , respectively.

### 3.4 Water Absorption

The results of water and buffered saline absorption are shown in Figures 3(C) and 3(D), respectively.

### 3.5 Degradation in Culture Medium

As shown in Figure 4(A), scaffolds without propolis (polyurethane, polyurethane/starch, and polyurethane/starch) lost 85-93% of their weight after three weeks of immersion, while scaffolds

containing propolis lost 84% of their weight after 30 days.

### 3.6 Surface Hydrophilicity

The surface hydrophilicity of the scaffolds was evaluated by measuring contact angles. Figure 4(B) shows the changes in contact angle with the addition of hyaluronic acid and propolis to the polyurethane/starch scaffold. The polyurethane scaffold had a contact angle of  $113.2^\circ$ , indicating hydrophobicity. The polyurethane/starch scaffold showed a lower contact angle of  $61.4^\circ$ , indicating increased surface hydrophilicity. The presence of hyaluronic acid further reduced the contact angle to  $42.8^\circ$ .

### 3.7 Thermal Properties

The thermal stability of the scaffolds was investigated using differential scanning calorimetry (DSC), and the results are shown in Figure 4(C).

### 3.8 Propolis Extract Release

Figure 4(D) shows the release profile of propolis from the polyurethane/starch/hyaluronic acid-propolis scaffolds at different propolis concentrations over the first 48 hours.

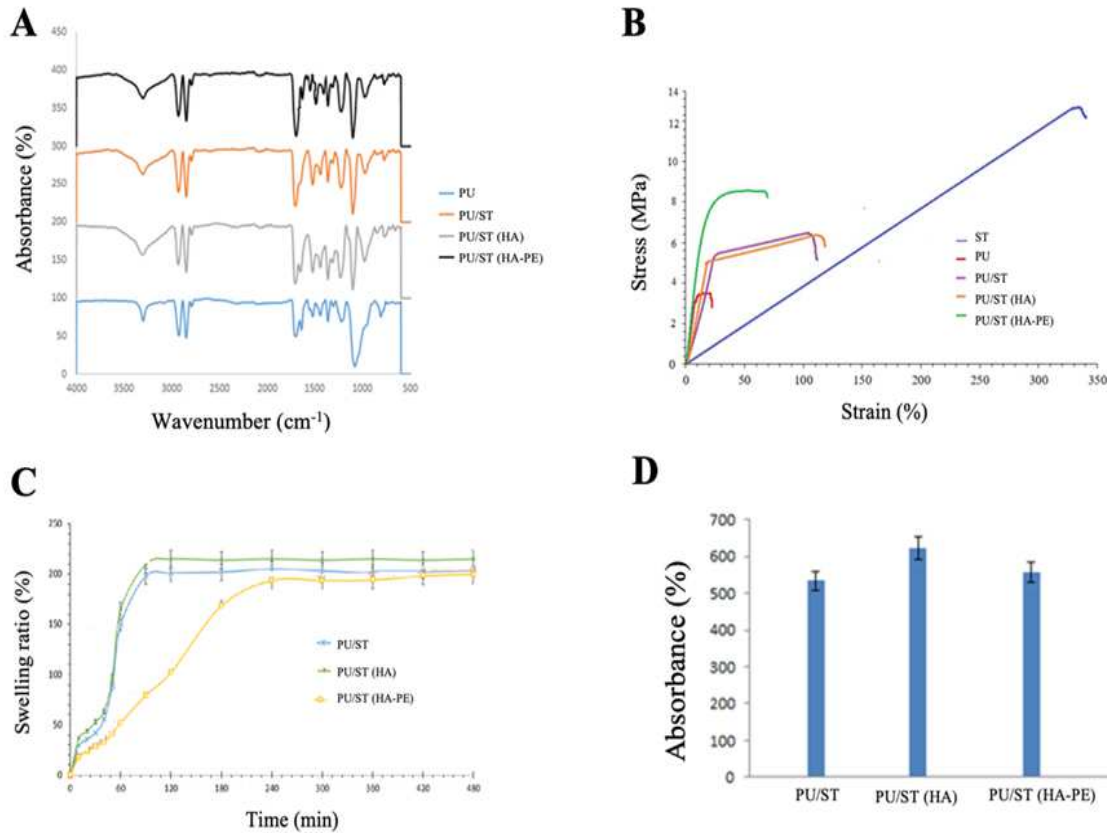


**Figure 3-** a) ATR-IR spectra of electrospun scaffolds. b) Stress-strain curves of electrospun nanofibers. c) Dynamic equilibrium swelling of scaffolds after 8 h. and d) PBS absorption of electrospun samples after 24 h of immersion in PBS solution at 37 °C.

### 3.9 Antibacterial activity

The antimicrobial properties of the scaffolds were tested against the starch bacteria *Staphylococcus aureus* and *Escherichia coli* using the agar diffusion method.

### 3.10 L929 Fibroblast Cell Survival and Proliferation

The proliferation of fibroblast cells on the electrospun scaffolds was evaluated using a cell viability assay. To assess cytotoxicity, the polyurethane, polyurethane/starch, polyurethane/starch, and polyurethane/starch/hyaluronic acid-propolis scaffolds were incubated with L929 cells for seven days.

### 3.11 Animal Studies

This study also evaluated the adhesion properties, cell proliferation, and wound healing effects of the scaffolds in adult male rats (Figure 6).

### 3.12 Histological Studies

Histological analysis showed that after 14 days, the number of hair follicles significantly increased in the scaffolds treated with electrospun samples compared to the control group. Furthermore, the number of blood vessels formed by day 14 was higher in the scaffold containing propolis compared to the control group.

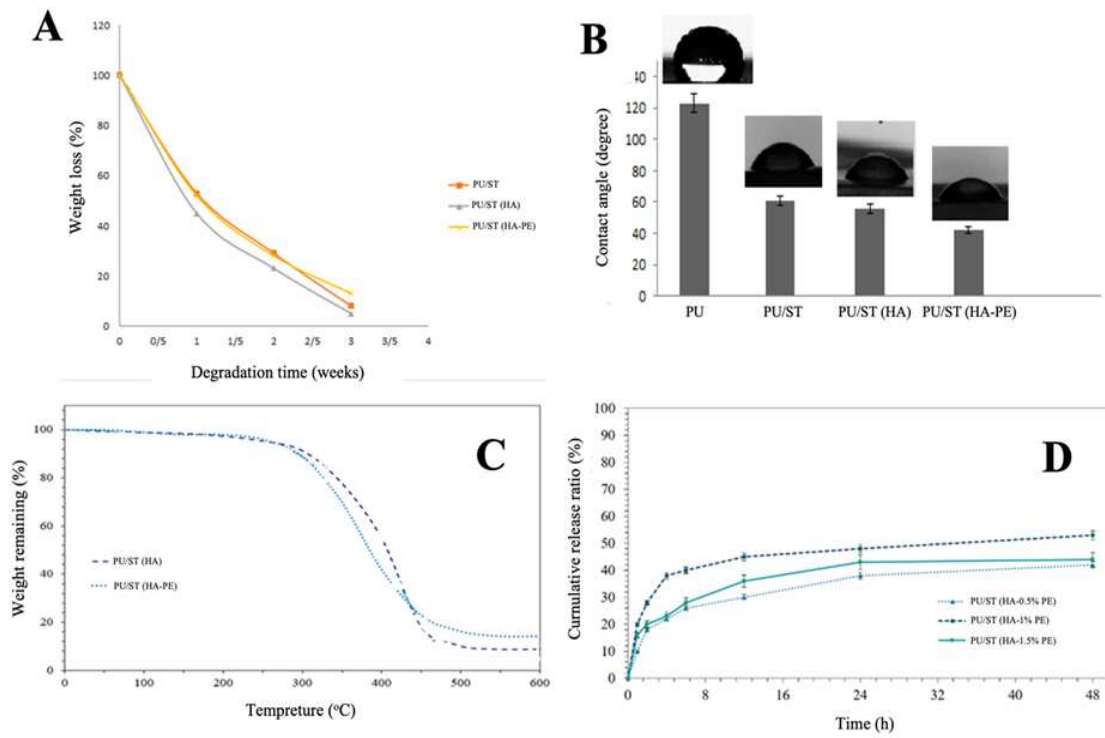


**Figure 4- a) Degradation profile of electrospun nanofibers. b) Water contact angles of nonwoven mats. c) Thermometric analysis of polyurethane/starch and polyurethane/starch/hyaluronic acid-propolis scaffolds. d) Release of propolis extract from electrospun core-shell nanofibers over 48 hours.**

**Table 3- Antimicrobial activity of electrospun fibers and commercial sample by zone of inhibition method.**

<i>Polyurethane/starch/hyaluronic acid</i>	<i>Polyurethane/starch/hyaluronic acid – propolis</i>	<i>Commercial sample</i>	<i>Microorganism</i>	<i>Restraint area (mm)</i>
-	0	0.14±5.37	<i>Escherichia coli</i>	0.63±1.04
-	0	0.12±5.89	<i>Staphylococcus aureus</i>	0.87±1.43

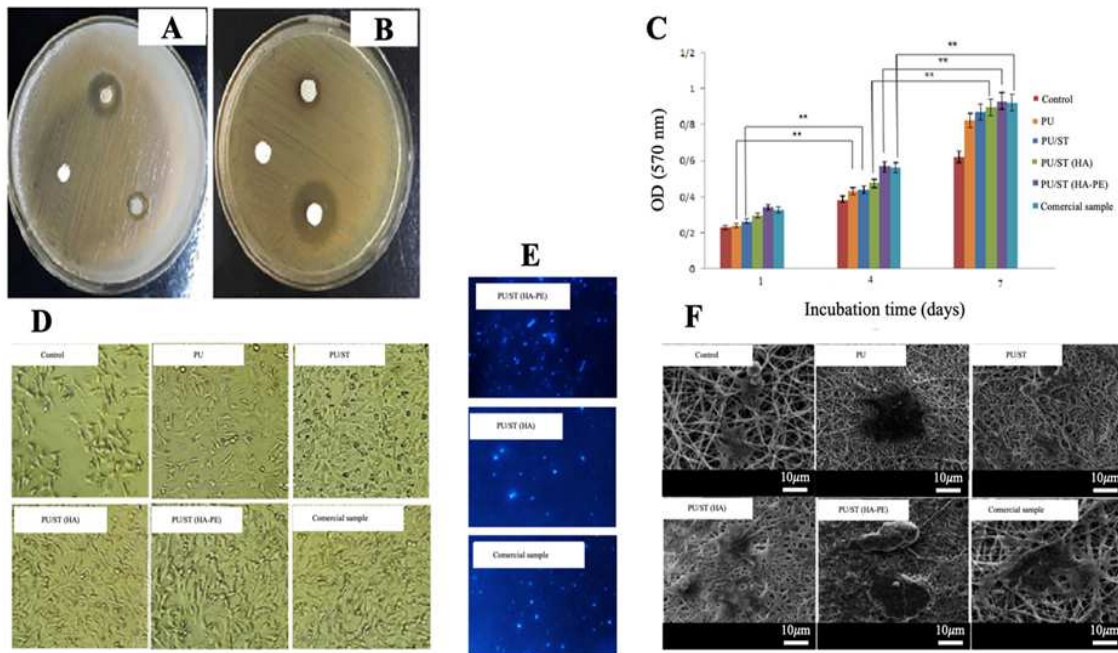


**Figure 5-** a) Inhibition zones of polyurethane/starch, polyurethane/starch/hyaluronic acid-propolis, and commercial scaffolds against *Staphylococcus aureus*. b) Inhibition zones of *Escherichia coli* after 24 hours of incubation. c) Cytotoxicity test results of polyurethane, polyurethane/starch, polyurethane/starch, polyurethane/starch/hyaluronic acid-propolis, and commercial scaffolds; d) Light microscope images of L929 cell growth on different scaffolds after four days of culture. Scanning electron microscope images of L929 fibroblast cells cultured on control and experimental scaffolds after four days.

## 4. Discussion

### 4.1 Morphological Characteristics

As shown in Figure 1, the polyurethane fibers have a uniform morphology with interconnected porosity and no bead formation. It is important to remember that electrospinning starch alone is a challenging process. For example, Salgado et al.<sup>46</sup> showed that starch fibers produced by electrospinning often encounter difficulties due to the complex polysaccharide chains in the natural polymer. These chains, along with hydrodynamic responses and repulsive forces in the solution, can negatively affect fiber formation and even block the needle tip, leading to discontinuous fibers. Similarly, Liu et al.<sup>28</sup> found that the surface tension of the starch solution can cause droplets to remain at the syringe tip during

electrospinning. In this study, a polyurethane solution (12 wt%) was used as the shell and a starch solution (9 wt%) as the core. The addition of propolis reduced the solution viscosity, allowing the formation of smaller fibers.<sup>47,48</sup> It was found that all electrospun scaffolds had a porosity of over 80% in the first layer, which is considered optimal for tissue engineering applications.

However, due to overlap, the porosity in the second and third layers was significantly reduced. The crosslinking process with glutaraldehyde vapor altered the scaffold structure, resulting in an insoluble form, as observed in Figure 2. Crosslinking helped maintain the scaffold porosity and prevented its collapse in an aqueous environment, which is consistent with the findings of Pieper et al.<sup>49</sup>

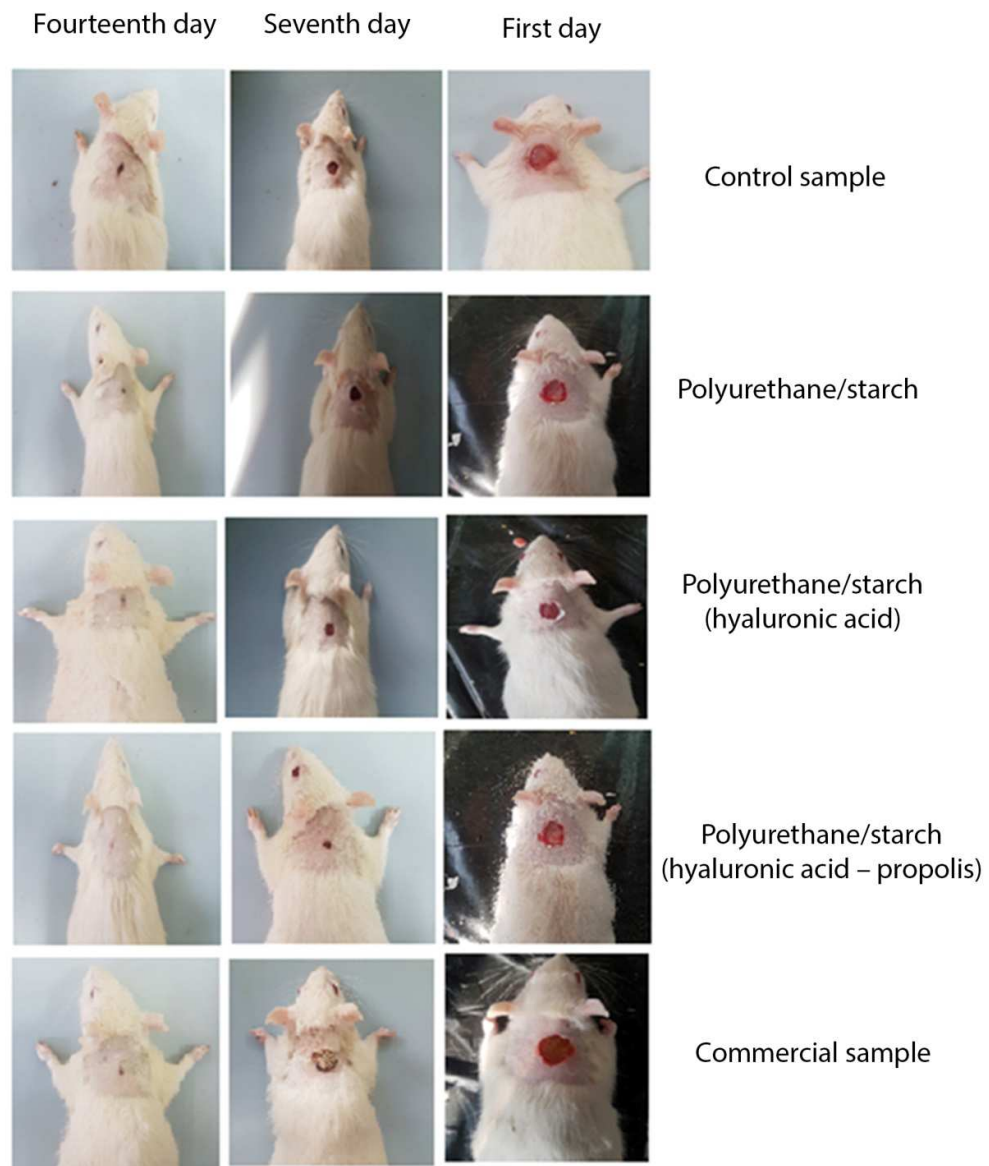


**Figure 6- Comparative images of the wound healing effect in different groups of core-shell structures and commercial groups.**

Transmission electron microscopy analysis confirmed the core-shell structure of the polyurethane/starch, polyurethane/starch, and polyurethane/starch/hyaluronic acid-propolis scaffolds. As shown in Figure 2(D), polyurethane fibers are loosely wrapped around the starch fibers, and there is a clear boundary between the core and shell. In all cases, the core flow rate was 0.135 mL/min, while the shell flow rate was 0.675 mL/min, confirming the formation of a core-shell structure in all electrospun samples. The addition of hyaluronic acid led to a decrease in fiber diameter and an increase in the shell-to-core ratio, as the anionic structure of hyaluronic acid generated an internal electric field that increased fiber stretching.<sup>50,51</sup> Furthermore, the presence of propolis in the core structure further defined the boundary between the core and shell. This phenomenon is attributed to the lower viscosity of the propolis solution compared to the polyurethane/starch and polyurethane/starch solutions.<sup>52</sup>

Similar results were reported by Surucu et al., who showed that in electrospun core-shell fibers, the core diameter is larger than the shell due to differences in material density.<sup>53</sup>

#### 4.2 ATR-FTIR

A characteristic absorption peak for pure starch appeared at 3393  $\text{cm}^{-1}$ , which corresponds to the hydroxyl band and complex stretching vibrations of free hydroxyl groups in the biopolymer structure. The peaks observed at 1369  $\text{cm}^{-1}$  were attributed to carbon-hydrogen-oxygen/carbon-carbon-hydrogen and carbon-oxygen-hydrogen bands, while the peaks at 1152 and 1027  $\text{cm}^{-1}$  correspond to the stretching of carbon-oxygen and carbon-carbon bonds, respectively.<sup>54,55</sup>

Additional peaks in the 1200-1500  $\text{cm}^{-1}$  range are related to the bending vibrations of carbon-hydrogen and oxygen-hydrogen bonds. For hyaluronic acid, the peaks observed at 1610-1630  $\text{cm}^{-1}$  and 945-955  $\text{cm}^{-1}$  were attributed to carboxylic acid groups. Also, the peaks at 1700-1650  $\text{cm}^{-1}$

and 3200-3500  $\text{cm}^{-1}$  are related to the stretching vibrations of the nitrogen-hydrogen bond.<sup>54,55</sup>

Regarding polyurethane, the peak at 3332  $\text{cm}^{-1}$  corresponds to the symmetric and asymmetric stretching vibrations of methylene.<sup>56</sup> For propolis, the peak at 1545  $\text{cm}^{-1}$  indicates the stretching vibrations of the nitrogen-hydrogen bond, while the peak at 1646  $\text{cm}^{-1}$  belongs to the C=O bond stretching. The peak at 2933  $\text{cm}^{-1}$  corresponds to the carbon-hydrogen stretching band of methylene groups, and hydroxyl and amine groups appeared at 3294  $\text{cm}^{-1}$ .<sup>57-62</sup>

#### 4.3 Mechanical Properties

The addition of polyurethane significantly improved the mechanical properties of the starch scaffold, with the polyurethane/starch core-shell scaffold achieving a tensile strength of  $7.93 \pm 0.17$  MPa and a strain at break of  $28 \pm 2\%$ . Similar findings have been reported by Yang et al. in their study on silk/hyaluronic acid scaffolds, where hyaluronic acid increased elasticity but decreased tensile strength.<sup>63,64</sup> However, in our study, the presence of propolis improved the scaffold strength while reducing elasticity, which confirms the results of Almedia et al., who observed similar behavior in collagen scaffolds with the addition of propolis for bone tissue engineering.<sup>65</sup>

#### 4.4 Water Absorption

Water absorption is a crucial feature for wound dressings and affects the scaffold's ability to absorb wound exudates and facilitate nutrient exchange. As shown in Figure 3(C), the swelling behavior of polyurethane/starch and polyurethane/starch scaffolds stabilized after 90 minutes, while the polyurethane/starch/hyaluronic acid-propolis scaffold reached equilibrium swelling after 240 minutes. The longer swelling time in propolis-containing scaffolds is attributed to the presence of hydrophobic amino acids in propolis.<sup>66</sup>

Figure 3(D) shows the PBS absorption capacity after 24 hours. The polyurethane/starch scaffold showed the highest absorption with a value of  $625 \pm 33\%$ , while the polyurethane scaffold absorbed only  $2.45 \pm 0.199\%$  water. The addition of propolis to the scaffolds slightly reduced PBS absorption, reaching  $7.73 \pm 0.558\%$ , likely due to the aromatic structure of flavonoids introducing some hydrophobicity.<sup>34</sup> A study by Al-Star et al. also reported that hyaluronic acid improves the swelling behavior of carrageenan-based scaffolds and increases water absorption through interactions between components.<sup>66</sup>

#### 4.5 Degradation in Culture Medium

To evaluate the degradation profile of the scaffolds, samples were immersed in PBS. Scaffold degradation is crucial in tissue engineering, as the scaffold must gradually degrade to facilitate new tissue formation.<sup>67</sup> The slower degradation rate observed in propolis-containing scaffolds could be due to the presence of flavonoids and other phenolic compounds in propolis, which act as hydrophobic agents. The addition of hyaluronic acid increased the degradability of the scaffold, which is consistent with the findings of Hopping et al., where hyaluronic acid-chitosan networks showed significant degradation after 4 weeks.<sup>68-70</sup>

#### 4.6 Surface Hydrophilicity

The decrease in the sample contact angle with the addition of hyaluronic acid is related to its functional groups (hydroxyl, carboxyl, and amine).<sup>71</sup> The increase in surface hydrophilicity with the addition of propolis is associated with an increase in surface energy, which has been linked to improved cell adhesion and proliferation, as shown by Lee et al.<sup>72,73</sup> These results indicate that polyurethane/starch/hyaluronic acid-propolis scaffolds can create favorable conditions for cell growth and attachment.

#### 4.7 Thermal Properties

The weight loss of the scaffolds was minimal at temperatures between 200-250°C, which may be attributed to the close

packing of polymer chains and the crystalline nature of the scaffolds. The addition of propolis slightly reduced the degradation rate, which may be attributed to the arrangement of polymer chains and the reduction in polymer crystallinity.<sup>74-77</sup>

#### 4.8 Propolis Extract Release

Propolis release was sustained in the first 24 hours, and a cumulative release of 41.3% was recorded for scaffolds containing 0.5% propolis by dry polymer weight. At higher propolis concentrations (1% and 1.5%), the cumulative release reached 79.4% and 55.6%, respectively. This release profile is desirable for promoting angiogenesis and wound healing in the early stages of recovery, especially for diabetic wounds where angiogenesis is impaired.<sup>78,79</sup>

#### 4.9 Antibacterial Properties

The polyurethane/starch scaffold did not exhibit significant antibacterial activity, while polyurethane/starch/hyaluronic acid-propolis scaffolds showed significant inhibition, with inhibition zone diameters of  $12.0 \pm 5.89$  mm for *E. coli* and  $0.63 \pm 1.04$  mm for *S. aureus*, respectively. The antibacterial effects of propolis are attributed to the presence of flavonoids and phenolic compounds, as well as fatty acids such as 10-hydroxy-2-decenoic acid, which are known for their antibacterial properties.<sup>80,81</sup>

Studies by Hong et al. and Melie et al. also confirm the antibacterial activity of these compounds.<sup>82-84</sup>

#### 4.10 L929 Fibroblast Cell Survival and Proliferation

As shown in Figure 5(C), none of the scaffolds exhibited toxicity. Notably, the polyurethane/starch/hyaluronic acid-propolis sample showed the highest cell growth rate, with a significant increase compared to the other groups ( $p < 0.05$ ). Among the other samples, the polyurethane/starch scaffold showed a greater increase in cell count compared to the pure polyurethane scaffold. Previous studies by Glomar et al.<sup>85</sup> have confirmed these results and suggested that the

physicochemical properties of starch, a natural polymer, contribute to L929 cell proliferation. Figure 5(D) also shows that the polyurethane/starch scaffold exhibited greater cell survival compared to polyurethane/starch, likely due to the hydration properties of hyaluronic acid, which supports fibroblast aggregation and reduces toxicity. Hyaluronic acid not only accelerates cell growth and induces tissue regeneration but also facilitates granulation tissue formation and wound epithelialization.<sup>86,87</sup> also observed similar results and noted that hyaluronic acid contributes to fibroblast proliferation and biological compatibility.

Among all the tested scaffolds, polyurethane/starch/hyaluronic acid-propolis showed the highest level of cell growth. The addition of propolis increased L929 cell proliferation, which is consistent with previous studies by Mona et al.<sup>88</sup>, who demonstrated propolis's ability to support cell growth. Hyaluronic acid and Rezade et al.<sup>89</sup> have also emphasized the positive effects of propolis on stem cell growth and differentiation in neural tissues.

Fluorescent images taken after one day of cell culture (Figure 5(E)) show strong cell adhesion to propolis-containing nanofibers. The polyurethane/starch/hyaluronic acid-propolis scaffold more effectively supported cell adhesion and survival compared to polyurethane/starch scaffolds and commercial scaffolds. These findings demonstrate the potential of propolis to enhance cell survival. SEM images taken after seven days of cell culture (Figure 5(F)) clearly show that fibroblast cells proliferated well and adhered to the polyurethane/starch and polyurethane/starch/hyaluronic acid-propolis scaffolds. The scaffold containing both hyaluronic acid and propolis provided a suitable substrate for fibroblast growth, while SEM images confirm significant cell penetration into the scaffold fibers. Overall, these results indicate that the combination of hyaluronic acid and propolis supports cell adhesion and proliferation, making these scaffolds suitable for tissue engineering applications.

#### 4.11 Animal Studies

Figure 6 shows that on day one, the wound surface in the scaffold-treated groups showed little difference compared to the control group. However, by days 7 and 14, these differences became significantly noticeable. The polyurethane/starch/hyaluronic acid-propolis group showed the most significant wound healing by day 14 and had a more pronounced difference compared to the control group.

#### 4.12 Histological Studies

Wound healing is a complex process involving four overlapping stages: coagulation, inflammation, fibroplasia, and tissue remodeling. Coagulation occurs due to vasoconstriction and the release of catecholamines. In the inflammatory phase, phagocytic cells infiltrate the wound. During fibroplasia, fibroblasts migrate to the wound site and produce collagen, which strengthens the wound, and angiogenesis begins. Finally, in the tissue remodeling stage, the tissue regains its natural structure.

Numerous studies have emphasized the antibacterial properties and healing effects of hyaluronic acid, particularly in the treatment of pressure ulcers. Opie et al.<sup>90</sup> reported that hyaluronic acid improves the epithelialization and vascularization processes at wound sites. Park et al.<sup>91</sup> showed that propolis accelerates wound healing by increasing collagen production and improving the healing process.

#### 4.13 Results of Variance Analysis and Post-Hoc Tests

This section presents the results of one-way analysis of variance (ANOVA) and post-hoc tests conducted to compare the groups with the control group. All data are reported as mean  $\pm$  standard deviation, and the significance level was set at  $p < 0.05$ .

##### 1. Analysis of Variance for Antimicrobial Activity

The antimicrobial activity of the samples was examined using the zone of inhibition test. The results for comparing the antibacterial activity of different samples

against *Staphylococcus aureus* and *Escherichia coli* bacteria are as follows:

- Starch: *Staphylococcus aureus*
- Polyurethane/starch/hyaluronic acid-propolis:  $12.8 \pm 0.53$  mm
- Polyurethane/starch:  $1.63 \pm 1.04$  mm
- Polyurethane/starch:  $7.93 \pm 0.02$  mm
- Control group: 0 mm

ANOVA results showed that the mean inhibition zones in different groups were significantly different ( $p < 0.001$ ). Dunnett's post-hoc test was used, which clearly showed the comparison between different groups and the control group. This comparison showed that the polyurethane/starch/hyaluronic acid-propolis combination had more antibacterial activity than the other groups.

- *Escherichia coli*
- Polyurethane/starch/hyaluronic acid-propolis:  $5.89 \pm 0.12$  mm
- Polyurethane/starch:  $1.63 \pm 1.04$  mm
- Polyurethane/starch:  $7.18 \pm 0.12$  mm
- Control group: 0 mm

Here, too, the ANOVA results showed a significant difference between the group means ( $p < 0.001$ ). The post-hoc test was again used and determined that the polyurethane/starch/hyaluronic acid-propolis group had a larger inhibition zone, especially when compared to the control group and other groups.

## 2. Analysis of Variance for Mechanical Properties

Mechanical properties, including tensile strength and elastic modulus, were examined as follows:

- Tensile Strength:
- Polyurethane:  $7.17 \pm 7.93$  MPa
- Polyurethane/starch:  $7.18 \pm 0.12$  MPa
- Polyurethane/starch:  $8.12 \pm 0.15$  MPa
- Polyurethane/starch/hyaluronic acid-propolis:  $8.62 \pm 0.10$  MPa

The results indicated a significant difference between the groups ( $p < 0.05$ ). According to the results of Dunnett's post-hoc test, it was clearly determined that polyurethane/starch/hyaluronic acid-

propolis had the highest tensile strength and therefore can be introduced as a suitable option for regenerative medical applications.

- Elastic Modulus:

The elastic modulus values were also examined and showed a significant difference between the groups ( $p < 0.05$ ). These findings emphasize the effect of the used compounds, leading to improved mechanical properties.

The results of the variance analysis show the direct effect of various compounds on the antimicrobial activity and mechanical properties of electrospun scaffolds. According to the results of post-hoc tests, such as Dunnett's test, we clearly observed significant differences between different groups and the control group. This research emphasizes the importance of selecting materials with optimal properties for developing efficient scaffolds in skin tissue engineering.

## 5. Conclusion

This study successfully developed core-shell nanofibrous scaffolds composed of polyurethane/starch loaded with propolis, fabricated at room temperature.

The resulting scaffolds exhibited excellent biopotential and hydrophilic properties, making them suitable candidates for medical applications, particularly in tissue engineering. The unique core-shell structure of the electrospun fibers facilitated sustained and controlled release of propolis at the wound site, which is crucial for enhancing therapeutic effects over an extended period. The scaffolds demonstrated a significant ability to accelerate the wound healing process, as evidenced by supporting epithelial cell proliferation and promoting epithelialization. The addition of propolis played a pivotal role in enhancing the regenerative properties of the scaffolds, contributing to the formation of granulation tissue and improved wound epithelialization. This effect was particularly evident in the polyurethane/starch/hyaluronic acid-propolis scaffolds, which showed effective performance in the early stages of wound care. In vivo experiments further emphasized

the potential of these scaffolds in promoting skin wound healing, with polyurethane/starch/hyaluronic acid-propolis nanofibers significantly improving healing compared to control groups. Cell adhesion, proliferation, and wound closure in these scaffolds indicate their strong potential as therapeutic options for advanced wound management.

Overall, this study highlights the potential of polyurethane/starch/hyaluronic acid-propolis core-shell nanofibrous scaffolds as promising materials for promoting rapid

and effective skin wound healing. Their ability to sustain the release of bioactive agents, coupled with their biopotential, makes these scaffolds valuable candidates for future clinical applications in tissue engineering and regenerative medicine. These scaffolds offer a novel approach to improving the quality and speed of wound healing, making them a versatile platform for treating various skin injuries. Further research and optimizations can pave the way for their application in more complex wound healing scenarios and broader medical fields.

## References:

1. Kolarsick, Paul AJ, Maria Ann Kolarsick, and Carolyn Goodwin. "Anatomy and physiology of the skin." *Journal of the Dermatology Nurses' Association* 3, no. 4 (2011): 203-213. DOI: 10.1097/JDN.0b013e3182274a98.
2. Rosli, Nur Liyana, Husniyati Roslan, Eshaifol Azam Omar, Norehan Mokhtar, Nor Hussaini Abdul Hapit, and Nornaimah Asem. "Phytochemical analysis and antioxidant activities of *Trigona Apicalis* propolis extract." In *AIP Conference Proceedings*, vol. 1791, no. 1. AIP Publishing, 2016. DOI: 10.1063/1.4968873.
3. Magro FILHO, Osvaldo, and Antonio César Perri de CARVALHO. "Application of propolis to dental sockets and skin wounds." *The Journal of Nihon University School of Dentistry* 32, no. 1 (1990): 4-13. DOI: 10.2334/josnusd1959.32.4.
4. Venus, M., J. Waterman, and I. McNab. *Basic physiology of the skin. Surgery (Oxford)*, 2010. 28(10): p. 469-472. DOI: <https://doi.org/10.1016/j.mpsur.2010.07.011>.
5. Ghatee, A., et al., Biomimetic nanocomposite scaffolds based on surface modified PCL-nanofibers containing curcumin embedded in chitosan/gelatin for skin regeneration. *Composites Part B: Engineering*, 2019. 177: 1-12. DOI: 10.1016/j.compositesb.2019.107339.
6. Celleno, L. and F. Tamburi, Structure and function of the skin, In *Nutritional Cosmetics*. 2009, Elsevier. p. 3-45. DOI: 10.1016/B978-0-8155-2029-0.50008-9.
7. Jiang, Xiaodong, Rachael A. Clark, Luzheng Liu, Amy J. Wagers, Robert C. Fuhlbrigge, and Thomas S. Kupper. "Skin infection generates non-migratory memory CD8+ TRM cells providing global skin immunity." *Nature* 483, no. 7388 (2012): 227-231. DOI: 10.1038/nature10851.
8. Chua, A.W.C., C.F. Saphira, and S.J. Chong. *Skin Tissue Engineering in Severe Burns: A Review on Its Therapeutic Applications, Regenerative Medicine and Plastic Surgery*. 2019, Springer. p. 117-136. DOI: 10.1007/978-3-030-19962-3-9.
9. Chua, Alvin Wen Choong, Yik Cheong Khoo, Bien Keem Tan, Kok Chai Tan, Chee Liam Foo, and Si Jack Chong. "Skin tissue engineering advances in severe burns: review and therapeutic applications." *Burns & trauma* 4 (2016). DOI: 10.1186/s41038-016-0027-y.
10. Kamel, Rami A., Joon Faii Ong, Elof Eriksson, Johan PE Junker, and Edward J. Caterson. "Tissue engineering of skin." *Journal of the American College of Surgeons* 217, no. 3 (2013): 533-555. DOI: 10.1016/j.jamcollsurg.2013.03.027.
11. Hendrickx, B., J.J. Vranckx, and A. Luttun, Cell-based vascularization strategies for skin tissue engineering. *Tissue Engineering Part B: Reviews*, 2011. 17(1): p. 13-24. DOI: 10.1089/ten.teb.2010.0315.
12. Shevchenko, R.V., S.L. James, and S.E. James, A review of tissue-engineered skin bioconstructs available for skin reconstruction. *Journal of the Royal Society Interface*, 2010. 7(43): p. 229-258. DOI: 10.1098/rsif.2009.0403.
13. Naahidi, Sheva, Mousa Jafari, Megan Logan, Yujie Wang, Yongfang Yuan, Hojae Bae, Brian Dixon, and P. Chen. "Bioco Mega Pascal tibility of hydrogel-based scaffolds for tissue engineering applications." *Biotechnology advances* 35, no. 5 (2017): 530-544. DOI: 10.1016/j.biotechadv.2017.05.006.
14. Salehi, Amin Orash Mahmoud, Saeed Heidari Keshel, Farshid Sefat, and Lobat Tayebi. "Use of polycaprolactone in corneal tissue engineering: A review." *Materials Today Communications* 27 (2021): 102402. DOI: 10.1016/j.mtcomm.2021.102402.
15. Jang, Jinah, Jongwan Lee, Young-Joon Seol, Young Hun Jeong, and Dong-Woo Cho. "Improving mechanical properties of alginate hydrogel by reinforcement with ethanol treated polycaprolactone nanofibers." *Composites Part B: Engineering* 45, no. 1 (2013): 1216-1221. DOI: 10.1016/j.compositesb.2012.09.059.
16. Salehi, Amin Orash Mahmoud, Mohammad Sadegh Nourbakhsh, Mohammad Rafienia, Alireza Baradaran-Rafii, and Saeed Heidari Keshel. "Corneal stromal regeneration by hybrid oriented poly ( $\epsilon$ -caprolactone)/lyophilized silk fibroin electrospun scaffold." *International Journal of Biological Macromolecules* 161 (2020): 377-388. DOI: 10.1016/j.ijbiomac.2020.06.045.
17. Bigham, Ashkan, Amin Orash Mahmoud Salehi, Mohammad Rafienia, Mohammad Reza Salamat, Shahram Rahmati, Maria Grazia Raucci, and Luigi Ambrosio. "Zn-substituted Mg 2SiO4 nanoparticles-incorporated PCL-silk fibroin composite scaffold: A multifunctional platform towards bone tissue regeneration." *Materials Science and Engineering: C* 127 (2021): 112242. DOI: 10.1016/j.msec.2021.112242.
18. Mi, Hao-Yang, Xin Jing, Brett N. Napiwocki, Breanna S. Hagerty, Guojun Chen, and Lih-Sheng Turng. "Biocoible, degradable thermoplastic polyurethane based on polycaprolactone- block- polytetrahydrofuran-block-polycaprolactone copolymers for soft tissue engineering." *Journal of Materials Chemistry B* 5, no. 22 (2017): 4137-4151. DOI: 10.1039/C7TB00419B.

19. Hong, Suk-Min, Jong-Wan Kim, Jonathan C. Knowles, and Myoung-Seon Gong. "Facile preparation of antibacterial, highly elastic silvered polyurethane nanofiber fabrics using silver carbamate and their dermal wound healing properties." *Journal of biomaterials applications* 31, no. 7 (2017): 1026-1038., DOI: 10.1177/0885328216687665.
20. Salama, Ahmed, and Mohamed El-Sakhawy. "Polysaccharides/propolis composite as promising materials with biomedical and packaging applications: A review." *Biomass Conversion and Biorefinery* 14, no. 4 (2024): 4555-4565. DOI: 10.1007/s13399-022-02814-5.
21. Chhabra, Roha, Vaibhavi Peshattiwar, Tejal Pant, Aparna Deshpande, Deepak Modi, Sadhana Sathaye, Anil Tibrewala, Sathish Dyawanapelly, Ratnesh Jain, and Prajakta Dandekar. "In vivo studies of 3D starch-gelatin scaffolds for full-thickness wound healing." *ACS Applied Bio Materials* 3, no. 5 (2020): 2920-2929., DOI: 10.1021/acsbm.9b01139.
22. Ounkaew, Artjima, Pornnapa Kasemsiri, Kaewta Jetsrisuparb, Hiroshi Uyama, Yu-I. Hsu, Thidarut Boonmars, Atchara Artchayasawat, Jesper TN Knijnenburg, and Prinya Chindaprasirt. "Synthesis of nanocomposite hydrogel based carboxymethyl starch/polyvinyl alcohol/nanosilver for biomedical materials." *Carbohydrate Polymers* 248 (2020): 116767., DOI: 10.1016/j.carbpol.2020.116767.
23. Tavakoli, Shima, Mahshid Kharaziha, Shervin Nemati, and Ali Kalateh. "Nanocomposite hydrogel based on carrageenan-coated starch / cellulose nanofibers as a hemorrhage control material." *Carbohydrate polymers* 251 (2021): 117013. DOI: 10.1016/j.carbpol.2020.117013.
24. Amal, B., B. Veena, V. P. Jayachandran, and Joy Shilpa. "Preparation and characterisation of Punica granatum pericarp aqueous extract loaded chitosan-collagen-starch membrane: role in wound healing process." *Journal of Materials Science: Materials in Medicine* 26 (2015): 1-9. DOI: 10.1007/s10856-015-5515-2.
25. Hemamalini, T. and V.R.G. Dev, Comprehensive review on electrospinning of starch polymer for biomedical applications. *International journal of biological macromolecules*, 2018. 106: p. 712-718. DOI: 10.1016/j.ijbiomac.2017.08.079.
26. Yang, Xiao, Wen Liu, Guanghui Xi, Mingshan Wang, Bin Liang, Yifen Shi, Yakai Feng, Xiangkui Ren, and Changcan Shi. "Fabricating antimicrobial peptide-immobilized starch sponges for hemorrhage control and antibacterial treatment." *Carbohydrate polymers* 222 (2019): 115012. DOI: 10.1016/j.carbpol.2019.115012.
27. Kanani, A.G. and S.H. Bahrami, Review on electrospun nanofibers scaffold and biomedical applications. *Trends Biomater Artif Organs*, 2010. 24(2): p. 93-115.
28. Liu, Guodong, Zhengbiao Gu, Yan Hong, Li Cheng, and Caiming Li. "Electrospun starch nanofibers: Recent advances, challenges, and strategies for potential pharmaceutical applications." *Journal of Controlled Release* 252 (2017): 95-107. DOI: 10.1016/j.jconrel.2017.03.016.
29. Kang, Y.O., J.N. Im, and W.H. Park, Morphological and permeable properties of antibacterial double-layered composite nonwovens consisting of microfibers and nanofibers. *Composites Part B: Engineering*, 2015. 75: p. 256-263. DOI: 10.1016/j.compositesb.2015.01.029.
30. Štateikė, Jurgita, and Rimvydas Milašius. "Influence of modified cationic starch in a mixed poly (vinyl alcohol)/cationic starch solution on the electrospinning process and web structure." *Autex Research Journal* 20, no. 1 (2020): 69-72. DOI: 10.2478/aut-2019-0010.
31. Koivusalo, Laura, Maija Kauppila, Sumanta Samanta, Vijay Singh Parihar, Tanja Ilmarinen, Susanna Miettinen, Oommen P. Oommen, and Heli Skottman. "Tissue adhesive hyaluronic acid hydrogels for sutureless stem cell delivery and regeneration of corneal epithelium and stroma." *Biomaterials* 225 (2019): 119516. DOI: 10.1016/j.biomaterials.2019.119516.
32. Wang, Tzu-Wei, Jui-Sheng Sun, Hsi-Chin Wu, Yang-Hwei Tsuang, Wen-Hsi Wang, and Feng-Huei Lin. "The effect of gelatin-chondroitin sulfate-hyaluronic acid skin substitute on wound healing in SCID mice." *Biomaterials* 27, no. 33 (2006): 5689-5697. DOI: 10.1016/j.biomaterials.2006.07.024.
33. Friedrich, E.E. and N.R. Washburn, Transport patterns of anti-TNF- $\alpha$  in burn wounds: Therapeutic implications of hyaluronic acid conjugation. *Biomaterials*, 2017. 114: p. 10-22. DOI: 10.1016/j.biomaterials.2016.11.003.
34. Viuda-Martos, M., Y. Ruiz-Navajas, J. Fernández-López, and J. A. Pérez-Álvarez. "Functional properties of honey, propolis, and royal jelly." *Journal of food science* 73, no. 9 (2008): R117-R124. DOI: 10.1111/j.1750-3841.2008.00966.x.
35. Da Rosa, Cristiano, Ian Lucas Bueno, Ana Clara Martins Quaresma, and Giovanna Barbarini Longato. "Healing potential of propolis in skin wounds evidenced by clinical studies." *Pharmaceuticals* 15, no. 9 (2022): 1143. DOI: 10.3390/ph15091143.
36. Xu, B., et al., Non-linear elasticity of core/shell spun PGS/PLLA fibres and their effect

- on cell proliferation. *Biomaterials*, 2013. 34(27): p. 6306-6317. DOI: 10.1016/j.biomaterials.2013.05.009.
37. Hadisi, Zhina, Mehdi Farokhi, Hamid Reza Bakhsheshi-Rad, Maryam Jahanshahi, Sadegh Hasanpour, Erik Pagan, Alireza Dolatshahi-Pirouz, Yu Shrike Zhang, Subhas C. Kundu, and Mohsen Akbari. "Hyaluronic acid (HA) based silk fibroin/zinc oxide core-shell electrospun dressing for burn wound management." *Macromolecular bioscience* 20, no. 4 (2020): 1900328. DOI: 10.1002/mabi.201900328.
  38. Xie, Xianrui, Yujie Chen, Xiaoyu Wang, Xiaoqing Xu, Yihong Shen, Ali Aldalbahi, Allison E. Fetz, Gary L. Bowlin, Mohamed El-Newehy, and Xiumei Mo. "Electrospinning nanofiber scaffolds for soft and hard tissue regeneration." *Journal of Materials Science & Technology* 59 (2020): 243-261. DOI: 10.1016/j.jmst.2020.04.037.
  39. Li, Wei, Nazim Cicek, David B. Levin, Sarvesh Logsetty, and Song Liu. "Bacteria-triggered release of a potent biocide from core-shell polyhydroxyalkanoate (PHA)-based nanofibers for wound dressing applications." *Journal of Biomaterials Science, Polymer Edition* 31, no. 3 (2020): 394-406. DOI: 10.1080/09205063.2019.1693882.
  40. Movahedi, Mehdi, Azadeh Asefnejad, Mohammad Rafienia, and Mohammad Taghi Khorasani. "Potential of novel electrospun core-shell structured polyurethane/starch (hyaluronic acid) nanofibers for skin tissue engineering: In vitro and in vivo evaluation." *International journal of biological macromolecules* 146(2020): 627-637. DOI: 10.1016/j.ijbiomac.2019.11.233.
  41. Afshar, Shahnoosh, Shiva Rashedi, Hossein Nazockdast, and Malihe Ghazalian. "Preparation and characterization of electrospun poly (lactic acid)-chitosan core-shell nanofibers with a new solvent system." *International journal of biological macromolecules* 138 (2019): 1130-1137. DOI: 10.1016/j.ijbiomac.2019.07.053.
  42. Man, Zhentao, Ling Yin, Zhenxing Shao, Xin Zhang, Xiaoqing Hu, Jingxian Zhu, Linghui Dai et al. "The effects of co-delivery of BMSC-affinity peptide and rhTGF- $\beta$ 1 from coaxial electrospun scaffolds on chondrogenic differentiation." *Biomaterials* 35, no. 19 (2014): 5250-5260. DOI: 10.1016/j.biomaterials.2014.03.031.
  43. Adeli, H., M.T. Khorasani, and M. Parvazinia, Wound dressing based on electrospun PVA/chitosan/starch nanofibrous mats: Fabrication, antibacterial and cytotoxicity evaluation and in vitro healing assay. *International journal of biological macromolecules*, 2019. 122: p. 238-254. DOI: 10.1016/j.ijbiomac.2018.10.115.
  44. Ye, Hongye, Kangyi Zhang, Dan Kai, Zhibiao Li, and Xian Jun Loh. "Polyester elastomers for soft tissue engineering." *Chemical Society Reviews* 47, no. 12 (2018): 4545-4580. DOI: 10.1039/C8CS00161H.
  45. Alhosseini, Sanaz Naghavi, Fathollah Moztafzadeh, Masoud Mozafari, Shadnaz Asgari, Masumeh Dodel, Ali Samadikuchaksaraei, Saeid Kargozar, and Newsha Jalali. "Synthesis and characterization of electrospun polyvinyl alcohol nanofibrous scaffolds modified by blending with chitosan for neural tissue engineering." *International journal of nanomedicine* (2012): 25-34. DOI: 10.2147/IJN.S25376#d1e181.
  46. Salgado, A., O.P. Coutinho, and R.L. Reis, Novel starch-based scaffolds for bone tissue engineering: cytotoxicity, cell culture, and protein expression. *Tissue engineering*, 2004. 10(3-4): p. 465-474. DOI: 10.1089/107632704323061825.
  47. Liu, Yang, Guiping Ma, Dawei Fang, Juan Xu, Hongwen Zhang, and Jun Nie. "Effects of solution properties and electric field on the electrospinning of hyaluronic acid." *Carbohydrate Polymers* 83, no. 2 (2011): 1011-1015. DOI: 10.1016/j.carbpol.2010.08.061.
  48. Doshi, Jayesh, and Darrell H. Reneker. "Electrospinning process and applications of electrospun fibers." *Journal of electrostatics* 35, no. 2-3 (1995): 151-160. DOI: 10.1016/0304-3886(95)00041-8.
  49. Pieper, J. S., A. Oosterhof, Pieter J. Dijkstra, J. H. Veerkamp, and T. H. Van Kuppevelt. "Preparation and characterization of porous crosslinked collagenous matrices containing bioavailable chondroitin sulphate." *Biomaterials* 20, no. 9 (1999): 847-858. DOI: 10.1016/S0142-9612(98)00240-3.
  50. Zhang, Kuihua, Linpeng Fan, Zhiyong Yan, Qiaozhen Yu, and Xiumei Mo. "Electrospun biomimetic nanofibrous scaffolds of silk fibroin/hyaluronic acid for tissue engineering." *Journal of Biomaterials Science, Polymer Edition* 23, no. 9 (2012): 1185-1198. DOI: 10.1163/092050611X576963.
  51. Chen, Guangkai, Junxia Guo, Jun Nie, and Guiping Ma. "Preparation, characterization, and application of PEO/HA core shell nanofibers based on electric field induced phase separation during electrospinning." *Polymer* 83 (2016): 12-19. DOI: 10.1016/j.polymer.2015.12.002.
  52. Heydari, Parisa, Jaleh Varshosaz, Anousheh Zargar Kharazi, and Saeed Karbasi. "Preparation and evaluation of poly glycerol sebacate/poly hydroxy butyrate core-shell electrospun nanofibers with sequentially release of ciprofloxacin and simvastatin in wound dressings." *Polymers for Advanced Technologies*

- 29, no. 6 (2018): 1795-1803. DOI: 10.1002/pat.4286.
53. Surucu, Seda, and Hilal Turkoglu Sasmazel. "Development of core-shell coaxially electrospun composite PCL/chitosan scaffolds." *International journal of biological macromolecules* 92 (2016): 321-328. DOI: 10.1016/j.ijbiomac.2016.07.013.
  54. Mano, J.F., D. Koniarova, and R. Reis. Thermal properties of thermoplastic starch/synthetic polymer blends with potential biomedical applicability. *Journal of materials science: Materials in medicine*, 2003. 14(2): p. 127-135. DOI: 10.1023/A: 1022015712170.
  55. Koski, C. and S. Bose, Effects of amylose content on the mechanical properties of starch-hydroxyapatite 3D printed bone scaffolds. *Additive Manufacturing*, 2019. 30: p. 100817. DOI: 10.1016/j.addma.2019.100817.
  56. Eskandarinia, Asghar, Amirhosein Kefayat, Mohammad Rafienia, Maria Agheb, Sepehr Navid, and Karim Ebrahimpour. "Cornstarch-based wound dressing incorporated with hyaluronic acid and propolis: In vitro and in vivo studies." *Carbohydrate polymers* 216 (2019): 25-35. DOI: 10.1016/j.carbpol.2019.03.091.
  57. Svečnjak, Lidija, Zvonimir Marijanović, Piotr Okińczyc, Piotr Marek Kuś, and Igor Jerković. "Mediterranean propolis from the adriatic sea islands as a source of natural antioxidants: Comprehensive chemical biodiversity determined by GC-MS, FTIR-ATR, UHPLC-DAD-QqTOF-MS, DPPH and FRAP assay." *Antioxidants* 9, no. 4 (2020): 337. DOI: 10.3390/antiox9040337.
  58. Lim, Jin Ru, Lee Suan Chua, and John Soo. "Study of stingless bee (*Heterotrigona itama*) propolis using LC-MS/MS and TGA-FTIR." *Applied Food Research* 3, no. 1 (2023): 100252. DOI: 10.1016/j.afres.2022.100252.
  59. Aziz, Saliha, Ali Akbar, Zareen Gul, Muhammad Bilal Sadiq, Jahangir Khan Achakzai, Nazir Ahmad Khan, Abdul Samad, Zia Ur Rehman, and Imran Ali. "Functional potential and chemical profile analysis of propolis oil extracted from propolis of balochistan." *Journal of Food Quality* 2022, no. 1 (2022): 4782813. DOI: 10.1155/2022/4782813.
  60. Sutjarittangtham, Krit, Sirikarn Sanpa, Tawee Tunkasiri, Panuwan Chantawannakul, Uraiwan Intatha, and Sukum Eitssayeam. "Bactericidal effects of propolis/polylactic acid (PLA) nanofibres obtained via electrospinning." *Journal of Apicultural Research* 53, no. 1 (2014): 109-115. DOI: 10.3896/IBRA.1.53.1.11.
  61. da Silva, Cleidiane, Anaclara Prasniewski, Matheus A. Calegari, Vanderlei Aparecido de Lima, and Tatiane LC Oldoni. "Determination of total phenolic compounds and antioxidant activity of ethanolic extracts of propolis using ATR-FT-IR spectroscopy and chemometrics." *Food Analytical Methods* 11 (2018): 2013-2021. DOI: 10.1007/s12161-018-1161-x.
  62. Siripatrawan, Ubonrat, and Waranya Vitchayakitti. "Improving functional properties of chitosan films as active food packaging by incorporating with propolis." *Food Hydrocolloids* 61 (2016): 695-702. DOI: 10.1016/j.foodhyd.2016.06.001.
  63. Balderas-Cordero, Daniela, Octavio Canales-Alvarez, Roberto Sánchez-Sánchez, Alejandro Cabrera-Wrooman, Maria Margarita Canales-Martinez, and Marco Aurelio Rodriguez-Monroy. "Anti-Inflammatory and Histological Analysis of Skin Wound Healing through Topical Application of Mexican Propolis." *International Journal of Molecular Sciences* 24, no. 14 (2023): 11831. DOI: 10.3390/ijms241411831.
  64. Yang, Wei, Hongjie Xu, Yong Lan, Qiyu Zhu, Yu Liu, Shaoshan Huang, Shengjun Shi, Andrei Hancharou, Bing Tang, and Rui Guo. "Preparation and characterisation of a novel silk fibroin/hyaluronic acid/sodium alginate scaffold for skin repair." *International journal of biological macromolecules* 130 (2019): 58-67. DOI: 10.1016/j.ijbiomac.2019.02.120.
  65. De Almeida, Enrik Barbosa, Juliana Cordeiro Cardoso, Adriana Karla de Lima, Nívia Lucas de Oliveira, Nicodemos Teles de Pontes-Filho, Sônia Oliveira Lima, Isana Carla Leal Souza, and Ricardo Luiz Cavalcanti de Albuquerque-Júnior. "The incorporation of Brazilian propolis into collagen-based dressing films improves dermal burn healing." *Journal of ethnopharmacology* 147, no. 2 (2013): 419-425. DOI: 10.1016/j.jep.2013.03.031.
  66. El-Aassar, M. R., G. F. El Fawal, Elbadawy A. Kamoun, and Moustafa MG Fouda. "Controlled drug release from cross-linked  $\kappa$ -carrageenan/hyaluronic acid membranes." *International Journal of Biological Macromolecules* 77 (2015): 322-329. DOI: 10.1016/j.ijbiomac.2015.03.055.
  67. Agheb, Maria, Mohammad Dinari, Mohammad Rafienia, and Hossein Salehi. "Novel electrospun nanofibers of modified gelatin-tyrosine in cartilage tissue engineering." *Materials Science and Engineering: C* 71 (2017): 240-251. DOI: 10.1016/j.msec.2016.10.003.
  68. Gunatillake, Pathiraja A., Raju Adhikari, and N. Gadegaard. "Biodegradable synthetic polymers for tissue engineering." *Eur Cell Mater* 5, no. 1 (2003): 1-16.
  68. Oellig, Claudia. "Acetonitrile extraction and dual-layer solid phase extraction clean-up for pesticide residue analysis in propolis." *Journal of Chromatography A* 1445 (2016): 19-26. DOI: 10.1016/j.chroma.2016.03.082.

69. Pastor, Clara, Laura Sánchez-González, Alicia Marcilla, A Mega Packal ro Chiralt, Maite Cháfer, and Chelo González-Martínez. "Quality and safety of table grapes coated with hydroxypropylmethylcellulose edible coatings containing propolis extract." *Postharvest Biology and Technology* 60, no. 1 (2011): 64-70. DOI: 10.1016/j.postharvbio.2010.11.003.
70. Wang, Wenyu, Xin Jin, Yonghao Zhu, Chengzhang Zhu, Jian Yang, Hongjie Wang, and Tong Lin. "Effect of vapor-phase glutaraldehyde crosslinking on electrospun starch fibers." *Carbohydrate polymers* 140 (2016): 356-361. DOI: 10.1016/j.carbpol.2015.12.061.
71. Mao, Jin Shu, Yu Ji Yin, and Kang De Yao. "The properties of chitosan-gelatin membranes and scaffolds modified with hyaluronic acid by different methods." *Biomaterials* 24, no. 9 (2003): 1621-1629. DOI: 10.1016/S0142-9612(02)00549-5.
72. Tan, Huaping, Constance R. Chu, Karin A. Payne, and Kacey G. Marra. "Injectable in situ forming biodegradable chitosan-hyaluronic acid based hydrogels for cartilage tissue engineering." *Biomaterials* 30, no. 13 (2009): 2499-2506. DOI: 10.1016/j.biomaterials.2008.12.080.
73. Lee, Eun Ji, Jong Ho Lee, Linhua Jin, Oh Seong Jin, Yong Cheol Shin, Sang Jin Oh, Jaebeom Lee, Suong-Hyu Hyon, and Dong-Wook Han. "Hyaluronic acid/poly (lactic-co-glycolic acid) core/shell fiber meshes loaded with epigallocatechin-3-O-gallate as skin tissue engineering scaffolds." *Journal of Nanoscience and Nanotechnology* 14, no. 11 (2014): 8458-8463. DOI: 10.1166/jnn.2014.9922.
74. Anjum, Aima Sameen, Eun Jong Son, Jae Hyung Yu, Inshik Ryu, Myung Soo Park, Chang Soon Hwang, Jae Woo Ahn, Joo Young Choi, and Sung Hoon Jeong. "Fabrication of durable hydrophobic porous polyurethane membrane via water droplet induced phase separation for protective textiles." *Textile Research Journal* 90, no. 11-12 (2020): 1245-1261. DOI: 10.1177/0040517519886059.
75. Trovati, Graziella, Edgar Ap Sanches, Salvador Claro Neto, Yvonne P. Mascarenhas, and Gilberto O. Chierice. "Characterization of polyurethane resins by FTIR, TGA, and XRD." *Journal of Applied Polymer Science* 115, no. 1 (2010): 263-268. DOI: 10.1002/app.31096.
76. Filip, Daniela, Doina Macocinschi, and Stelian Vlad. "Thermogravimetric study for polyurethane materials for biomedical applications." *Composites Part B: Engineering* 42, no. 6 (2011): 1474-1479. DOI: 10.1016/j.compositesb.2011.04.050.
77. Ahire, J. J., D. Robertson, D. P. Neveling, A. J. Van Reenen, and L. M. T. Dicks. "Hyaluronic acid-coated poly (d, l-lactide) (PDLLA) nanofibers prepared by electrospinning and coating." *Rsc Advances* 6, no. 41 (2016): 34791-34796. DOI: 10.1039/C6RA01996J.
78. Arnold, Frank, and David C. West. "Angiogenesis in wound healing." *Pharmacology & therapeutics* 52, no. 3 (1991): 407-422. DOI: 10.1016/0163-7258(91)90034-J.
79. Duscher, Dominik, Evgenios Neofytou, Victor W. Wong, Zeshaan N. Maan, Robert C. Rennert, Mohammed Inayathullah, Michael Januszyk "Transdermal deferoxamine prevents pressure-induced diabetic ulcers." *Proceedings of the National Academy of Sciences* 112, no. 1 (2015): 94-99. DOI: 10.1073/pnas.1413445112.
80. Kim, Jeong In, Hem Raj Pant, Hyun-Jaung Sim, Kang Min Lee, and Cheol Sang Kim. "Electrospun propolis/polyurethane composite nanofibers for biomedical applications." *Materials Science and Engineering: C* 44 (2014): 52-57. DOI: 10.1016/j.msec.2014.07.062.
82. Huang WenZhe, Huang WenZhe, Dai XiaoJun Dai XiaoJun, Liu YanQing Liu YanQing, Zhang ChaoFeng Zhang ChaoFeng, Zhang Mian, Zhang Mian, and Wang ZhengTao Wang ZhengTao. "Studies on antibacterial activity of flavonoids and diarylheptanoids from *Alpinia katsumadai*." (2006): 37-40.
81. Fujiwara, Suguru, Jiro Imai, Mineko Fujiwara, Tomoko Yaeshima, Takuji Kawashima, and Kumpei Kobayashi. "A potent antibacterial protein in royal jelly. Purification and determination of the primary structure of royalisin." *Journal of biological chemistry* 265, no. 19 (1990): 11333-11337. DOI: 10.1016/S0021-9258(19)38596-5.
82. Marei, N., Development of chitosan 2D film scaffolds and nanoparticles enriched with royal jelly and grape seed extract: Enhanced antibacterial and wound healing activity. 2018.
83. Waghmare, Vijaya Sadashiv, Pallavi Ravindra Wadke, Sathish Dyawanapelly, Aparna Deshpande, Ratnesh Jain, and Prajakta Dandekar. "Starch based nanofibrous scaffolds for wound healing applications." *Bioactive materials* 3, no. 3 (2018): 255-266. DOI: 10.1016/j.bioactmat.2017.11.006.
84. Voinchet, Véronique, Pascal Vasseur, and Jérôme Kern. "Efficacy and safety of hyaluronic acid in the management of acute wounds." *American journal of clinical dermatology* 7 (2006): 353-357. DOI: 10.2165/00128071-200607060-00003.
85. Liu, Haifeng, Jinshu Mao, Kangde Yao, Guanghui Yang, Lei Cui, and Yilin Cao. "A study on a chitosan-gelatin-hyaluronic acid scaffold as artificial skin in vitro and its tissue engineering applications." *Journal of Biomaterials Science, Polymer Edition* 15, no. 1 (2004): 25-40. DOI: 10.1163/156856204322752219.

86. El-Gayar, Mona H., Khaled M. Aboshanab, Mohammad M. Aboulwafa, and Nadia A. Hassouna. "Antivirulence and wound healing effects of royal jelly and garlic extract for the control of MRSA skin infections." *Wound Medicine* 13 (2016): 18-27. DOI: 10.1016/j.wndm.2016.05.004.
87. Ebrahimie, M., S. Asgharzadieh, H. Shirzad, N. Ebrahimie, M. Hoseini, and M. Rafieian-kopaei. "An evaluation of the influence of royal jelly on differentiation of stem cells into neuronal cells invitro." *Journal of Babol University of Medical Sciences* 18, no. 3 (2016): 38-44 .
88. Uppal, Rohit, Gita N. Ramaswamy, C. Arnold, Robert Goodband, and Y. Wang. "Hyaluronic acid nanofiber wound dressing-production, characterization, and in vivo behavior." *Journal of Biomedical Materials Research Part B: Applied Biomaterials* 97, no. 1 (2011): 20-29. DOI: 10.1002/jbm.b.31776.
89. Park, Hye Min, Eunson Hwang, Kwang Gill Lee, Sang-Mi Han, Yunhi Cho, and Sun Yeou Kim. "Royal jelly protects against ultraviolet B-induced photoaging in human skin fibroblasts via enhancing collagen production." *Journal of medicinal food* 14, no. 9 (2011): 899-906. DOI: 10.1089/jmf.2010.1363.